

ISBN 978-83-945717-8-8

Conference proceedings  
**Transport Problems 2019**

XI INTERNATIONAL  
SCIENTIFIC  
CONFERENCE  
26.06-28.06 2019  
Katowice  
Bochnia

VIII INTERNATIONAL  
SYMPOSIUM OF YOUNG  
RESEARCHERS  
24.06-25.06 2019  
Katowice



Silesian  
University  
of Technology

UNDER THE HONORARY PATRONAGE OF MAYOR OF  
KATOWICE CITY  
AND RECTOR OF SILESIAN UNIVERSITY OF TECHNOLOGY



Faculty of Transport  
Silesian University of Technology

Silesian University of Technology  
Faculty of Transport



# Transport Problems 2019

## Proceedings

XI International Scientific Conference

VIII International Symposium of Young Researchers

UNDER THE HONORARY PATRONAGE OF MAYOR OF KATOWICE CITY  
AND RECTOR OF SILESIAN UNIVERSITY OF TECHNOLOGY



Silesian University  
of Technology

ISBN 978-83-945717-8-8

Transport Problems  
International Scientific Journal

*editor-in-chief*  
**A. Sładkowski**  
*editorial board*

*P. Czech, M. Cieśla, T. Haniszewski,  
M. Juzek, W. Kamiński, P. Marzec, G. Wojnar*

*CONFERENCE -  
TABLE OF  
CONTENTS*

*SYMPOSIUM -  
AUTHORS LIST*

*CONFERENCE -  
AUTHORS LIST*

*CONFERENCE &  
SYMPOSIUM  
PROGRAM*

*SYMPOSIUM -  
TABLE OF  
CONTENTS*

*CONFERENCE &  
SYMPOSIUM  
PROCEEDINGS*

*CONFERENCE &  
SYMPOSIUM  
PARTICIPANTS*

No.	Author, Title	Pages	
		Begin	End
	Eugen ROSCA, Aura RUSCA, Cristina OPREA <i>Evaluating the traffic impacts of new constructions to an urban area based on microsimulation</i>		
66	Florin RUSCA, Mihaela POPA, Eugen ROSCA, Aura RUSCA, Mircea ROSCA, Oana DINU <i>Assessing the transit capacity of port shunting yards through discrete simulation</i>	<a href="#">594</a>	604
67	Marcin RYCHTER, Piotr SUŁEK <i>Analysis of violations in digital recording devices in the aspect of the security of the digital tachograph system</i>	<a href="#">605</a>	613
68	Katarzyna SICIŃSKA, Agnieszka KRUPIŃSKA <i>SaferWheels: investigation on scene of an accident with powered two-wheeler and bicycle, results of data</i>	<a href="#">614</a>	625
69	Gergana STANEVA, Kamelia DIMITROVA, Rosen IVANOV, Georgy KADIKYANOV <i>Sound level study of hybrid car</i>	<a href="#">626</a>	635
70	Ondrej STOPKA, Mária STOPKOVÁ, Vladimír ĽUPTÁK, Srećko KRILE <i>Application of the selected multi-criteria decision-making methods to identify the autonomous train system supplier in the selected company</i>	<a href="#">636</a>	645
71	Bakyt SYZDYKBAYEVA, Zhanarys RAIMBEKOV, Assel BAIMBETOVA <i>The functioning of freight and commercial logistics distribution systems (for example, macro-regions and agglomerations of Kazakhstan)</i>	<a href="#">646</a>	661
72	Bożena SZCZUCKA-LASOTA, Tomasz WĘGRZYN, Agnieszka KURC-LISIECKA, Adam JUREK, Maciej LESZCZYŃSKI <i>Welding of car construction elements made from aluminum alloy</i>	<a href="#">662</a>	673
73	Igor TARAN, Vadim LITVIN <i>Determination of rational parameters for urban bus route in combined mode</i>	<a href="#">674</a>	689
74	Igor TARAN, Iryna KLYMENKO <i>Distribution the power flows in a closed contour of HSMT in the process of mine locomotive braking</i>	<a href="#">690</a>	701
75	George TUMANISHVILI, Tamaz NATRIASHVILI, Aleksander SLADKOWSKI, Tengiz NADIRADZE <i>Influence of the third body of the railway transport running gear interacting elements on their tribological properties</i>	<a href="#">702</a>	711
76	Asliddin UROKOV, Muzaffar MAMATKULOV <i>Impact of microclimate in exploiting highways</i>	<a href="#">712</a>	715
77	Gediminas VAIČIŪNAS, Stasys STEIŠŪNAS,	<a href="#">716</a>	725

**Keywords:** third body, rolling, sliding, friction, contact zone

**George TUMANISHVILI\***, **Tamaz NATRIASHVILI**,  
**Aleksander SLADKOWSKI**, **Tengiz NADIRADZE**

Institute of Machine Mechanics  
10 Mindeli, 0186 Tbilisi, Georgia

\*Corresponding author. E-mail: ge.tumanishvili@gmail.com

## **INFLUENCE OF THE THIRD BODY OF THE RAILWAY TRANSPORT RUNNING GEAR INTERACTING ELEMENTS ON THEIR TRIBOLOGICAL PROPERTIES**

**Summary.** The instability of tribology properties of interacting surfaces of the railway transport running gear provokes the vibrations, noise and high rate of various kinds of wear and other undesirable phenomena. These properties, especially the friction coefficient and wear rate vary in the wide range and there are not the reliable methods for their prediction and control that complicates solution of various problems.

The dependence of variation of tribological properties of the interacting surfaces on the properties and destruction degree of the third body was ascertained experimentally. The slip speed and load have especially great influence on the destruction of the third body. The tribological properties of the contact zone and instability of the friction coefficient change sharply at the progressive destruction of the third body. The signs of beginning and development of destruction of the third body and its laws are revealed in the laboratory conditions that can be used as a basis for prediction of tribological properties of these surfaces.

As supposed reasons of the wheel sliding on the rail are cited a movement of the wheelset in the curve, a wheelset with the wheels of different diameters and a wheelset with one elliptical wheel. The mechanisms of the wheel sliding on the rail for these cases are explained.

### **1. INTRODUCTION**

It is difficult to predict and control the friction forces, wear rate of various types, vibrations and noise of the heavy loaded interacting surfaces of the railway transport running gear that decreases traffic safety, increases energy losses on friction etc. Many works are devoted to the researches into dependences of the tribological properties on the various factors [1-5], though their mechanisms of generation and variation are not always clear that complicates revelation of the parameters influencing them [6, 7].

There are many reasons of generation of vibrations and noise at movement of the train, part of which are well studied, predictable and ways of their decrease are known. The interacting surfaces of wheels and rails are characterized by the various types of irregularities: 5-20 mm gaps in the rail joints where the rail tread surfaces are spaced by 0.5-2 mm in the vertical direction; the various wear traces (rail corrugation, fatigue etc.) and various deviations from the wheel roundness, are the sources of vibrations and noise.

The wheels and rails interaction is accompanied by the forced and self-excited vibrations of various frequencies [8-12]. As the main reason of the forced vibrations is considered macro- and micro-asperities of the rail (periodic and separate asperities) and the friction between the wheel and rail is thought the source of the self-vibrations. It must be noted that to various working conditions of

the heavy loaded contacting surfaces and wear types correspond typical for them micro-asperities which can be different from the initial micro-asperity [13]. The researches have shown an important role of the tread and steering surfaces in generation of the vibrations (self-vibrations) and noise, whose reasons are not studied sufficiently. There is quite vague information on the reasons of the self-vibrations generated at interaction of the wheel and rail [8].

The generation of vibrations in the contact zone of the heavy loaded interacting elements of the railway transport running gear are stipulated by the complex processes proceeding in the contact zone: as a result of interaction of surfaces with the environment, they are coated by the layers of various physical and chemical origins that are the components of the third body in the contact zone and have a great influence on the tribological properties of the contacting surfaces. According to observations by Godet, dry friction is largely determined not by the properties of friction materials of the contacting pair, but by the characteristics of the structure and composition of the thin film that is formed on the surfaces of both bodies because of compaction of the wear product, its chemical composition and oxidation. Destination of the third body in the tribological systems is separation of the contacting surfaces, providing with the stable friction forces of proper values and protection of the surfaces against damage of various types. Tribological properties of the third body greatly depend on the initial properties of its component elements and features of the contact zone. The sliding velocity, power and thermal loading and the sliding distance have especially great influence on the destruction of the third body. For providing the stability of the third body in the contact zone of the wheels and rails and reduction of the derailment probability, energy consumed on traction, environment pollution and maintenance expenses, the decrease of the sliding distance and relative sliding is especially important.

The rail-wheel squeal in curves is the most common type of vibrations and noise. It is especially typical for high-speed movements, when because of various reasons the relative sliding and sliding distance increase. This contributes destruction of the third body, seizure of the surfaces at direct contact, subsequent destruction of the seized surfaces and instability of the friction forces and relative movement of surfaces.

Many negative phenomena (wear, noise, vibrations) are generated because of the wheel sliding on the rail. For elimination of the wheel sliding in the curves, the wheel tread surface is given a conical form with the intention of making the outer wheel to roll on the greater diameter passing the greater distance than the inner wheel and rotate both wheels through the equal angles, maintaining this way radial position of the wheelset axle. However, this intention can be realized only for a certain combination of such parameters, as are radius of the rail-track curvature, mass and speed of the rolling stock, friction coefficient between the wheel and rail, etc. Therefore, practically the outer wheel rolls on the less diameter than necessary and in the case of the free wheelset (without bogie), it falls behind the inner wheel, inclining the wheelset axle from the radial position.

In the case of the non-free wheelset, the bogie makes the wheelset maintain a radial position, forcing the outer wheel to roll the greater distance not to fall behind the inner wheel. Thereat, the outer wheel rotates through the greater angle than the inner one and the wheelset axle is twisted. The angle of twist of the wheelset can increase up to the value that is stipulated by the friction force between the wheel and rail. When this angle of twist reaches the limited value the wheel slides on the rail due to action of the wheelset axle elastic moment tending to bring it back to the equilibrium position.

Similarly, the wheel will slide on the rail at rolling in the straight rail-track of the wheelset with the wheels of different diameters or with one wheel having an elliptical form. The mechanisms of the wheel sliding on the rail for the three noted cases are considered and explained in the next paragraphs.

## 2. MOVEMENT OF THE WAGON WHEELSET IN THE CURVE

At pure rolling of the free wheelset (without bogie) in the curved rail-track with radius of curvature  $R$  of the internal rail, its axle will be inclined from radial position because both wheels will have passed equal distances  $l$ . However, in the wagon wheel-set rolling with velocity  $V$ , the outer wheel is constraint to maintain the radial position and pass greater distance  $l+\Delta l$ , rotating relative to

the inner wheel in the clockwise direction if it is seen from axial direction A (Fig. 1). At that, the wheel-set axle is twisted through angle  $\varphi$  equal to the ratio of the difference  $\Delta l$  of the outer and inner arcs to the radius  $D/2$  of the wheel tread surface, supposing that the both wheels are rolling on the tread surfaces of equal diameters:

$$\varphi = 2\Delta l / D \quad (1)$$

From the drawing  $\alpha = l/R = (l + \Delta l)/(R + \Delta R) = \Delta l / \Delta R$ ,  
where

$$\Delta l = l\Delta R / R, \quad (2)$$

and therefore

$$\varphi = 2l\Delta R / DR. \quad (3)$$

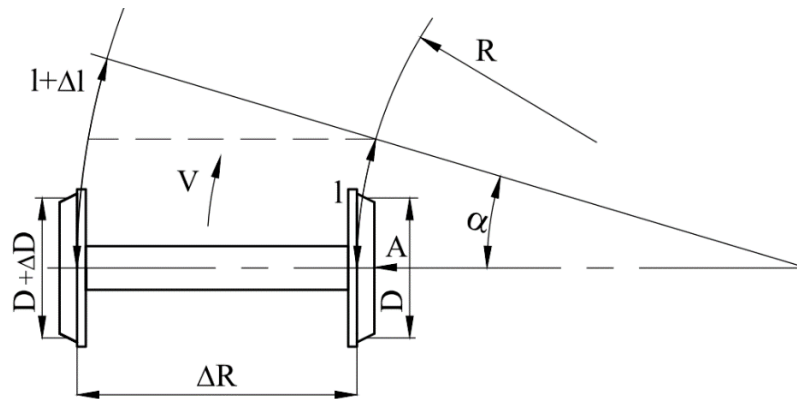


Fig. 1. Movement of the wagon wheel-set in the curve

On the other hand, the maximum angle of twist of the wheel-set axle  $\varphi_{\max}$  depends on the friction force

$$F = fQ \quad (4)$$

and is calculated by the known from the resistance of materials, formula

$$\varphi_{\max} = ML / I_p G, \quad (5)$$

where  $M$  is a torque caused by the friction force

$$M = FD/2 = fQD/2; \quad (6)$$

$f$  – friction coefficient;  $Q$  – vertical load (half of the load on the wheel-set) of the wheel on the rail;  $L$  – length of the wheel-set axle;  $I_p$  – polar moment of inertia of the wheel-set axle cross section;  $G$  – modulus of rigidity (shear modulus) of the axle material.

We determine distance between the worn out segments of the rail or path  $l$  (at travelling this path the wheels are rolling on the rail without sliding), at rolling of which the axle is twisted on the maximum angle  $\varphi_{\max}$ , from (3) replacing  $\varphi$  by  $\varphi_{\max}$ :

$$l = DR \varphi_{\max} / 2\Delta R = MLDR / 2I_p G \Delta R \quad (7)$$

and putting the found  $l$  into (2) we obtain difference of the paths passed by the outer and inner wheels at which the axle is twisted on the maximum angle  $\varphi_{\max}$

$$\Delta l = MLD / 2I_p G. \quad (8)$$

### 3. MOVEMENT OF THE WAGON WHEELSET WITH THE WHEELS OF DIFFERENT DIAMETERS IN THE STRAIGHT RAIL-TRACK

At rolling of the free wheel-set (without bogie) with the wheels of different diameters  $D$  and  $D + \Delta D$  in the straight rail-track the distance  $l$ , the greater wheel passes a greater distance  $l + \Delta l$ , deflecting the wheel-set axle from its perpendicular position relative to the rail track (Fig. 2a). But in the wagon wheel-set the axle being constraint to retain perpendicular position the smaller wheel is forced to pass the same distance  $l + \Delta l$  and rotate relative to the greater wheel in the clockwise

direction, if it is seen from axial direction A. At that, the wheel-set axle is twisted through angle  $\varphi$  that is determined by formula (1), from where, considering (5) we obtain the value of  $\Delta l$  (see formula (8)) corresponding to the maximum angle of twist  $\varphi_{max}$ .

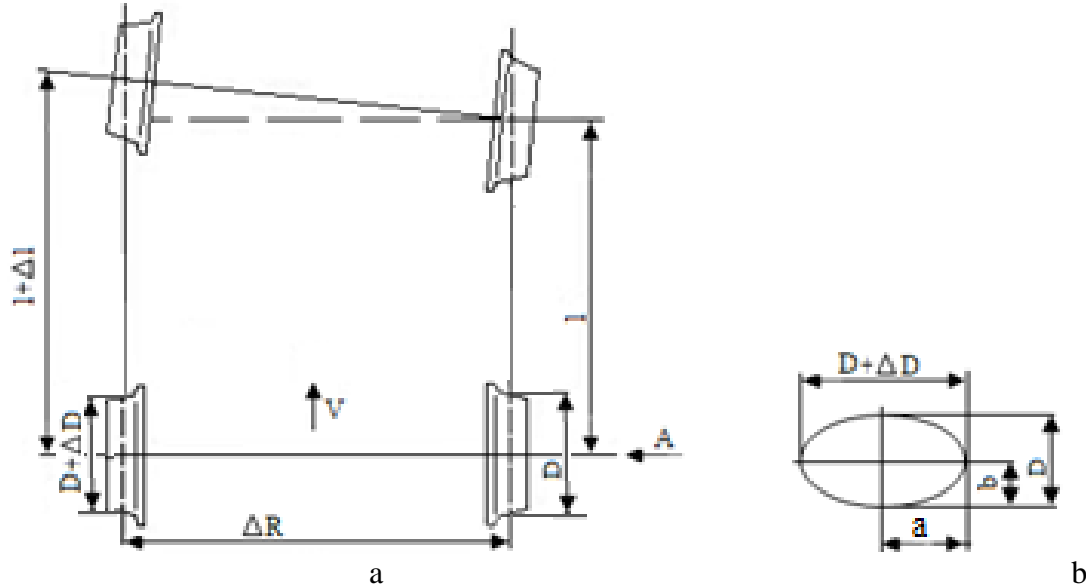


Fig. 2. Movement of the free wheel-set in the straight rail-track: a) with the wheels of different diameters or with one elliptical wheel; b) parameters of ellipticity

The following proportion can be written from the drawing:  $(l+\Delta l)/l = (D+\Delta D)/D$  or  $\Delta l/l = \Delta D/D$ , from which we obtain distance  $l$  between the worn-out segments at passing of which the wheel-set axle will be twisted through angle  $\varphi_{max}$ :

$$l = \Delta l D / \Delta D = MLD^2 / 2I_p G \Delta D \tag{9}$$

#### 4. MOVEMENT OF THE WAGON WHEELSET WITH ONE ELLIPTICAL WHEEL IN THE STRAIGHT RAIL-TRACK

Consider a free wheel-set with one wheel of diameter  $D$  and other elliptical wheel with the small  $D$  and bigger  $D+\Delta D$  diameters moving in the straight rail-track (Fig. 2a,b).

At one revolution, these wheels will pass the different distances, correspondingly  $l$  and  $l+\Delta l$ , deflecting the wheel-set axle from its perpendicular position relative to the rail-track (Fig. 2a). However, in the wagon wheel-set the axle being constraint to retain perpendicular position, the wheel with diameter  $D$  is forced to pass the same (greater) distance  $l+\Delta l$  and rotate relative to the elliptical wheel in the clockwise direction if it is seen from axial direction A. At that, the wheel-set axle is twisted through angle  $\varphi$  that is determined by formula (1).

The difference of distances passed by the wheels at one revolution is  $\Delta l = L - \pi D$ , where the length of the elliptical tread surface

$$L = \pi [3(a+b) - (3a+b)(a+3b)] \tag{10}$$

or

$$\Delta l = \pi [3(a+b) - (3a+b)(a+3b)] - \pi D \tag{11}$$

The value  $\Delta l^I$  corresponding to maximum angle of twist  $\varphi_{max}$  is obtained considering formula (5)

$$\Delta l^I = \varphi_{max} D / 2 = MLD / 2I_p G \tag{12}$$

The distance  $l$  at passing of which the wheel-set axle will be twisted on the angle  $\varphi_{max}$  will be then

$$l = \pi D \Delta l^I / \Delta l \tag{13}$$

In all the three cases considered above, at removing or decrease of the torque  $M$  acting on the wheel that takes place at its vertical vibrations when the friction force  $F$  decreases, the angle of twist of



the axle will start to decrease. Suppose  $\varphi_{\max}$  falls down to zero during time  $t$ . This will take place at rotation of the inner wheel in the clockwise direction relative to the outer wheel on the angle  $\varphi_{\max}$  since the flange of the outer wheel is pressed on the rail and the friction force arisen between the flange and rail additionally restricts its movement. Obviously, during this time  $t$  the inner wheel will roll and slide simultaneously on the rail and the rolling and sliding distance on the rail will be

$$S_r = Vt \tag{14}$$

We note that the rolling and sliding distance on the wheel tread surface is

$$S_w = \Delta l + S_r$$

or for the variant of the elliptical wheel

$$S_w = \Delta l^I + S_r \tag{15}$$

where  $\Delta l$  or  $\Delta l^I$  is a sliding friction path and the wavelength of the worn-out rail (Fig. 3)

$$W = l + S_r \tag{16}$$

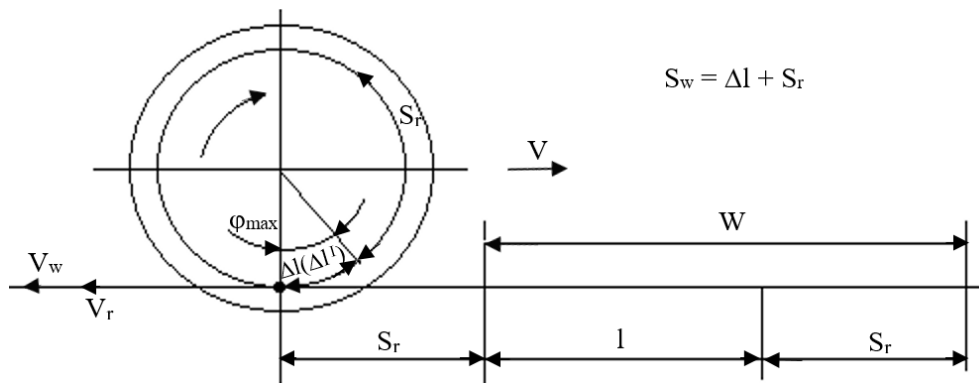


Fig. 3. The rolling and sliding distances on the rail and wheel

This value of the wavelength assumes that at release of the inner wheel the friction force acting on it from the rail is zero. When the friction force differs from zero the wavelength will be less since its both components will decrease and its value depends on the friction force magnitude.

To determine time  $t$  we present the wheel-set as a one-mass torsional vibratory system (Fig. 4a), where  $C$  is the torsional rigidity of the wheel-set axle,  $I$  – total moment of inertia of the inner wheel. Then, angle of twist  $\varphi_{\max}$  will fall down to zero in conformity with a law of free vibrations of this vibratory system during the period  $P/4$  (Fig. 4b).

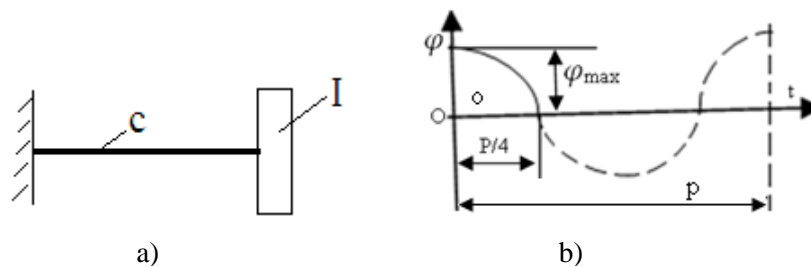


Fig. 4. a) One-mass torsional vibratory system; b) Graph of the system free vibrations

At that, period of free vibrations

$$P = 2\pi\sqrt{I/C} \tag{17}$$

and consequently, time  $t$  will be

$$t = P/4 = \frac{\pi}{2}\sqrt{I/C} \tag{18}$$

The average velocity of the wheel contact point relative to the wheel center (Fig. 5)

$$V_w = -\frac{D\varphi_{\max}}{2t} + V_r \tag{19}$$

where  $V_r = -V$  is a velocity of the rail contact point relative to the wheel center.

We note that maximum velocity of the wheel contact point relative to the wheel center

$$V_w^I = -\frac{A\omega D}{2} + V_r = -\varphi_{\max}\sqrt{\frac{C}{I}} \times \frac{D}{2} + V_r \quad (19^I)$$

where  $A = \varphi_{\max}$  is an amplitude of the wheel-set shaft torsion vibrations;  $\omega = \sqrt{C/I}$  - cyclic frequency of vibrations.

Sliding velocity

$$V_{sl} = V_w - V_r \quad (20)$$

Relative sliding velocities

$$K_r = \frac{V_{sl}}{V_r} \times 100\% \quad \text{and} \quad K_w = \frac{V_{sl}}{V_w} \times 100\% \quad (21)$$

The depth of the worn-out layer a year of the rail segment  $S_r$

$$h = i\Delta IN \quad (22)$$

where  $i$  is the wear intensity and  $N$  – number of cycles which is determined as follows

$$N = N_1 N_2 N_3 N_4 \quad (23)$$

where  $N_1$  is a number of the trains passing by a day;  $N_2$  – number of wagons in the train;  $N_3$  – number of wheels on one side of the wagon;  $N_4$  – number of days a year.

## 5. THE EXPERIMENTAL RESEARCHES INTO BEHAVIOUR OF TRIBOLOGICAL PROPERTIES OF THE CONTACT ZONE

Despite the considerable quantity of works, devoted to study of behavior of tribological properties of the heavy loaded interacting surface of rails, wheels and brake shoes, as well as other interacting surfaces, the proper results are not obtained yet.

To fill the gaps, we carried out the experimental researches on the twin disk machine MT1. The researches were performed at rolling of discs with sliding up to 20% (Fig. 5a) and at pure slip, imitating operation of the wheel and brake shoe (Fig. 5). The rollers imitating the wheel and rail had diameters of 40 mm and widths of 10 and 12 mm. The tests were performed at single application of the friction modifier on the rolling surface of the roller. After certain number of revolutions, a thin layer of the friction modifier was destroyed that was revealed by sharp increase of the friction moment and initial signs of scuffing on the surfaces. Without repeated feeding of the friction modifier, the damage process was progressed. The rollers with various degrees of damage are shown in Fig. 5: b) with initial signs of damage; c) damage in the form of a narrow strip; d) damage of the whole contacting area.

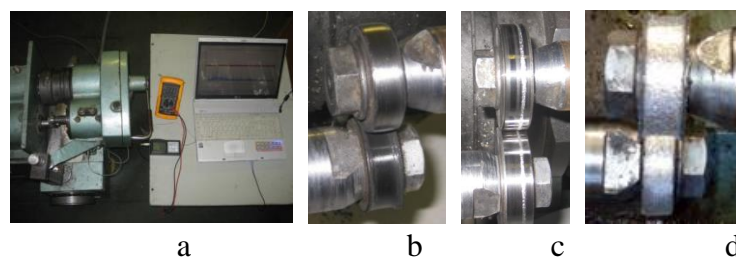


Fig. 5. The twin disk machine MT1 (a) and stages of damage of the interacting surfaces: b) damage in the separate points; c) damage in the form of the narrow strip; d) damage on the whole area of the contacting surfaces

In Fig. 6 are shown the operating member of the twin disk machine and experimental samples of the brake shoe.

The experimental samples, a disk with diameter of 50 mm and width 12 mm was made from steel 45 and a brake shoe has been cut out from the wagon brake shoe. The experiments were carried out at 1000 rev/min and contact pressure (1 – 2) MPa. Before the experiment, the friction modifier was applied on the contacting surface of the disk. Although the number of the variable parameters in

such experiments is limited, it can give us a qualitative picture of the brake pads working capacity. As for a quantitative information, the field tests will be necessary for its obtaining.

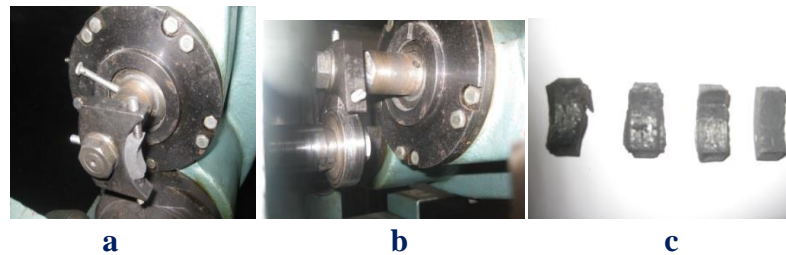


Fig. 6. An operating member of the twin disk machine and experimental samples of the brake shoe: a) brake shoe mounted in the slot of the machine; b) experimental sample in the process of the test; c) experimental samples after tests

Artificial separation of the interacting surfaces by the third body is not usually used in the friction brakes and their interacting surfaces are not protected from direct interaction.

When there is a friction modifier between the interacting surfaces, they are not in direct contact and thus the friction force is in this case formed by the shear between the layers of the third body. Because of this the contact pressure is distributed more evenly, that can unload the interacting surfaces and decrease the destruction rate (Fig. 7).

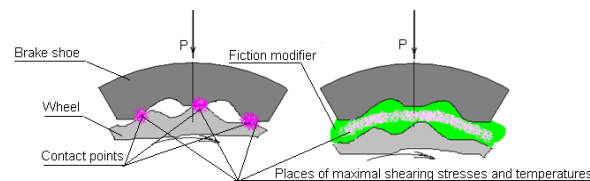


Fig. 7. Interaction of the brake shoe and disk at presence and lack of the friction modifier in the contact zone

The phenomenon of seizure is typical for interacting surfaces. This may occur if the seizing surfaces are juvenile (free from dirty, oxide films and adsorbed layers) and are approached to the inter-atomic distance [7]. With time, the number of such places may increase until formation of the continuous zones of seizure. The atoms lying on the crystal surface are surrounded by the less number of the neighboring atoms, than the atoms inside the crystal, and therefore, they possess some excess of free energy and are disposed to form additional connections with other atoms that turn out to be near the juvenile surface. At approached juvenile surfaces close enough, as a result of interaction between atoms of the seizing crystals, the energy-stable configurations of electrons are formed that correspond to the system minimal potential energy in comparison with the atoms inside the crystals.

The main demand imposed on the wheel/rail and friction brake interacting surfaces materials is a providing of the stable friction forces with proper values of longevity of the interacting surfaces. The friction factor varies in the wide range that causes increase of the damage rate of the interacting surfaces, auto-vibrations and noise. Our experimental researches have shown that variation of the friction coefficient, wear rate and damage type depend on the relative sliding velocity (creep, slip), contributing destruction of the third body, and a degree of destruction of the third body. In Fig. 8 are shown dependences of the friction coefficient and damage types (wear rate) on the creep, slip and relative sliding velocity.

The continuous and initial (restorable) destruction of the third body provides the stable (or with small impulses) “negative friction”. Destruction of the third body in the multiple places (in the broken narrow strips) leads to a certain increase of the friction moment and to “neutral friction”. The irreversible destruction of the third body leads to spacious damage of the third body, adhesive junction of micro-asperities, disruption of these junctions and increase of the friction forces (“positive friction”) (Fig. 8a).

In Fig. 8b are shown dependences of the damage types (wear rate) on the slip, where the mild and severe wear rates correspond to the low relative sliding velocity and continuous or initial destruction of the third body, while the catastrophic damage type corresponds to the multiple and progressive destruction of the third body.

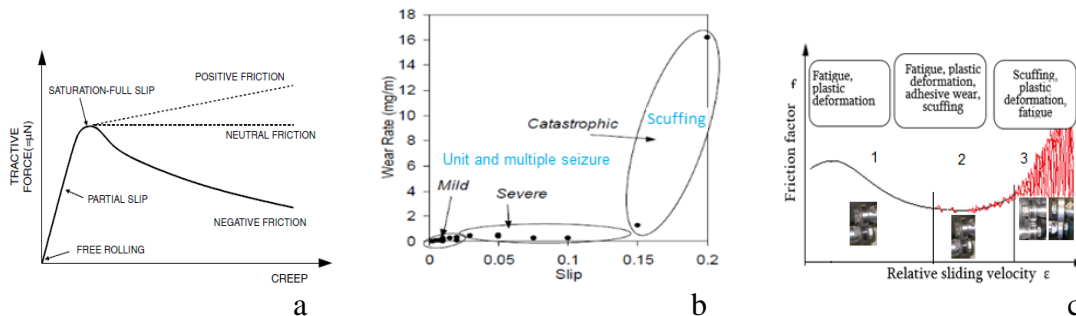


Fig. 8. Dependence of the tractive force (friction coefficient) on the creep (a) [2, 4]; dependence of damage types on the slip (b) [15] and dependence of the friction coefficient on the relative sliding velocity (c)

At certain conditions, the third body undergoes to progressive irreversible destruction. In Fig. 8c is shown dependence of the friction coefficient on the relative sliding velocity, increase of which causes the increase of destruction degree of the third body; the types of damage at various destruction degree of the third body are shown also.

As it is seen from the Fig. 8 the negative, neutral and positive behaviours of the friction forces, as well as the mild, severe and catastrophic wear and types of damage of the interacting surfaces are stipulated by the properties and degree of destruction of the third body.

The dependences of the wear types (rates) on the relative sliding velocity are shown in Fig. 8b. The middle and severe wear rates are not greatly differing from each other and when the sliding velocity exceeds a certain value, a highly intensive catastrophic wear begins.

The three zones can be distinguished in Fig 8c. At low relative sliding speed, full separation of the interacting surfaces and continuous third body provide high wear resistance of the interacting surfaces and relatively stable friction coefficient (zone 1 Fig. 8c). In such conditions, the main damage types are the fatigue and plastic deformations and the zone "mild" in Fig. 8b corresponds to zone 1 in Fig. 8c. The small-scale increase of the sliding speed leads to appearance of small damage sources in multiple places and emergence of small splashes of the friction moment (zone 2, Fig. 8c). The typical damage types of this zone are fatigue, plastic deformation, adhesive wear and limited rate of scuffing and the zone "sever" in Fig. 8b corresponds to zone 2 in Fig. 8c. At further increase of the relative sliding speed, destruction of the third body becomes irreversible and extending, and multiple seizures become uninterrupted (causing scuffing), propagating on the whole width of the interacting surfaces. The corresponding wear becomes "catastrophic" and the zone of the same name in Fig. 8b corresponds to zone 3 in Fig. 8c.

Therefore, we have the three stages of the wear: wear at continuous third body; wear at reversible discontinuous third body and wear at irreversible discontinuous third body. The first stage is characterized by the stable friction coefficient and minimal wear rate; the second stage does not greatly differ from the first one; a sharp increase of the friction coefficient in the contact zone at the third stage indicates beginning of the irreversible (progressive) destruction of the third body and is characterized by sharp instability of the friction factor and catastrophic wear rate.

In terms of tribological characteristics, zones 1 and 2 indicate the acceptable working conditions of the tribological system and can provide its improved running ability. In contrast to this, zone 3 is characterized by the sharp increase of the value and instability of the friction coefficient, wear rate ("catastrophic wear"), vibrations and noise and operation in this zone is inadmissible. In this zone, the rate of the "catastrophic" wear depends on the properties of interacting surfaces and third body also that should be considered at its prediction.

## 6. CONCLUSIONS

- Variation of the friction coefficient as well as other tribological properties of interacting surfaces depends on the properties and degree of destruction of the third body;
- The friction coefficient, its stability and beginning of destruction of the third body can be ascertained in the laboratory by the wear traces on the laboratory samples. The rise of the third body destruction, is clearly reflected in the oscillogram of the friction moment, obtained in the laboratory conditions, allowing prediction of the third body destruction;
- The mechanisms of the wheel sliding on the rail at movement of the wheelset in the curve and geometrical deviations of one of the wheels are explained.

## References

1. Lewis, R. & Olofsson, U. (Eds.) *Wheel–Rail Interface Handbook*. Cambridge, UK: Woodhead Publishing Limited. 2009. 307 p.
2. Eadie, D.T. & Kalousek, J. & Chiddik, K.C. The role of high positive friction (HPF) modifier in the control of short pitch corrugations and related phenomena. *Wear*. 2002. Vol. 253. No. 1-2. P. 185-192.
3. Ślădkowski, A. & Sitarz, M. Analysis of wheel-rail interaction using FE software. *Wear*. 2005. Vol. 258. No. 7-8. P. 1217-1223.
4. Eadie, D.T. & Bovey, E.D. & Kalousek, J. The role of friction control in effective management of wheel/rail interface. In: *Railway Technology Conference at Radix*. Birmingham, UK. 2002. P. 221-228.
5. Chiddick, K.S. & Eadie, D.T. Wheel/rail friction management solutions. In: *14 Int. Conference on Current Problems in Rail Vehicles "PRORAIL 99"*. Prague. 1999.
6. Eadie, D.T. & Santoro, M. Top-of-rail friction control for curve noise mitigation and corrugation rate reduction. *Journal of Sound and Vibration*. 2006. Vol. 293. No. 3-5. P. 747-757.
7. Mo, Y. & Turner, K.T. & Szlufarska, I. Friction laws at the nanoscale. *Nature*. 2009. Vol. 457(7233). P. 1116-1119.
8. Кудинов, В.А. Динамика станков. Москва: Машиностроение, 1967. 360 с. [In Russian: Kudinov, V.A. Dynamics of metal cutting machines. Moscow: Engineering].
9. Кудинов, В.А. & Лисицын, Н.М. Основные факторы, влияющие на равномерность перемещения столов и суппортов станков при смешанном трении. *Станки и инструмент*. 1962. № 2. С. 1-5. [In Russian: Kudinov, V.A. & Lisicin, N.M. The main factors impacting the evenness of the table displacement in the lathe support at the mixed friction. *Machines and tools*].
10. Blok, H. Fundamental Mechanical Aspects of Boundary Lubrication. *SAE Transactions*. 1940. Vol. 35. No. 1. P. 54-68.
11. *Railroad Safety Statistics*, Annual Report 2002. U.S. Department of transportation, Federal Railroad Administration.
12. Крагельский, И.В. *Трение и износ*. 2-е изд. Москва: Машиностроение, 1968. 430 с. [In Russian: Kragelski, I.V. *Friction and wear*. Moscow: Engineering]
13. Семенов, А.П. О теории схватывания металлов. В сб.: *Теория трения и изнашивания*. Москва: Наука. 1965. С.164-170. [In Russian: Semenov, A.P. On the theory of the setting of metals. In Proc.: *Theory of friction and wear*. Moscow: Science].
14. Lewis, R. & Olofsson, U. Mapping rail wear regimes and transitions. *Wear*. 2004. Vol. 257. No. 7-8. P. 721-729.

15. Lewis, R. & Dwyer-Joyce, R.S. Wear mechanisms and transitions in railway wheel steels. *Proceedings of the Institution of Mechanical Engineers, Part J: Journal of Engineering Tribology*. 2004. Vol. 218. No. 6. P. 467-478.